Diabatic errors in Majorana braiding with bosonic bath

Amit Nag and Jay D. Sau

Phys. Rev. B **100**, 014511 — Published 12 July 2019

DOI: 10.1103/PhysRevB.100.014511

Diabatic errors in Majorana braiding with bosonic bath

Amit Nag[1] and Jay D. Sau[1]

[1]*Condensed Matter Theory Center and Joint Quantum Institute, Department of Physics, University of Maryland, College Park, Maryland 20742-4111, USA*

(Dated: June 24, 2019)

Majorana mode based topological qubits are potentially subject to diabatic errors that in principle can limit the utility of topological quantum computation. Using a combination of analytical and numerical methods we study the diabatic errors in Majorana-based topological Y-junction that are coupled to a Bosonic bath in the Markovian approximation. We find that in the absence of a bath, the error can be made exponentially small with increasing braiding time, only when the time-variation in the Hamiltonian is completely smooth. The presence of a dominantly dissipative Markovian bath is found to eliminate this exponential scaling of error to a power-law scaling as T^{-1} with T being the braiding time. However, the inclusion of relaxation improves this scaling slightly to go as T^{-2}. Thus, coupling of topological systems to Bosonic baths can lead to powerlaw in braiding time diabatic errors that might limit the speed of topologically protected operations using Majorana modes.

I. INTRODUCTION

Non-Abelian states are the building blocks of topological quantum-computation as these states carry non-locally encoded quantum information immune to decoherence[4]. One class of such non-Abelian states are Majorana zero modes (MZMs) that emerge naturally as the ground-state of (effective) p-wave superconductors[5,6]. MZMs (and non-Abelian states in general) appear as degenerate ground states of a Hamiltonian forming a ground state subspace that is topologically protected by a gap[5,6]. In its simplest form such a degeneracy involves the appearance of two localized MZMs at the ends of a topological superconducting nanowire[5–8]. In such systems quantum information can be encoded in the fermion parity of the degenerate ground state which depend on the occupation/non-occupation of non-local Dirac fermion mode formed out of the pair of localized MZMs. While the non-locally encoded quantum information is protected against environmental decoherence[4,9], excitation rate due to finite temperature is exponentially suppressed as long as the temperature is smaller than the ground state energy gap. Concrete theoretical proposals to realize MZMs in solid-state systems[7,8] have led to substantial experimental efforts to realize MZMs. Encouraging experimental progress in this direction in the recent years[10–17] has motivated new set of theoretical proposals that outline basic architecture of quantum gates to be realized following specific protocols to move and manipulate MZMs in order to braid and exchange a set of MZMs with each other[2,3,18,19].

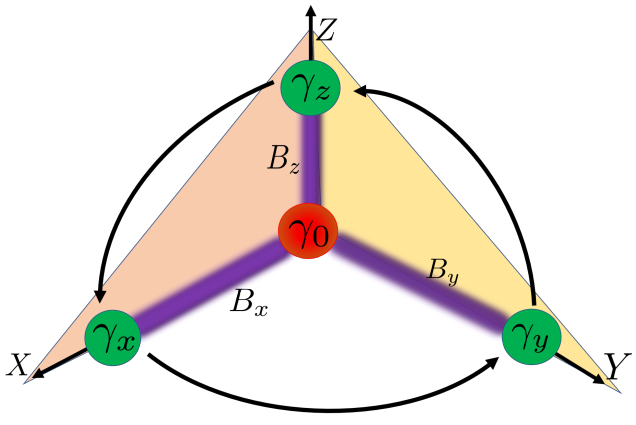

FIG. 1: (Color Online) Schematic description of the time-dependence of the braiding Hamiltonian(Eq. 1) using the protocol in Ref.[1–3]. The parameter B_α represents the coupling of Majoranas γ_α and γ_0. The topological degeneracy of the spectrum of the system is guaranteed by the requirement that at least one component of $\vec{B} = (B_x, B_y, B_z)$ vanishes. Braiding is accomplished by successive rotations about the vanishing direction chosen to be x, y and z. The Bosonic bath considered here is assumed to couple as fluctuations of $B_{x,y,z}$.

Despite the excitement regarding the possibility of exponentially small error in topological qubits realized from MZMs, most of the studies of the protection of MZMs have been in the static limit. A less studied question is the protection of quantum information stored in MZMs to diabatic errors resulting from the finite speed of operations[20–23]. Specifically, one might worry that since the topological phase of matter is a ground state property, finite gate speed might have an effect of taking the system out of the ground state in a way that introduces errors. This issue has been raised in some studies of the dynamics of braiding[23] that suggest the use of a measurement based protocol as a possible way to avoid such diabatic errors. In contrast key-board based braiding protocols[18] seem to reduce some of the diabatic errors and find error rates that scale exponentially in the rate of the process[24,25]. Another potentially critical ingredient in MZM braiding is the interaction of the MZMs with a Bosonic bath. MZMs in equilibrium turn out to be robust to the coupling to Bosonic baths[9,26–28] since thermal equilibrium ensures that the population of excited states is exponentially small at vanishing temperature. In contrast, recent studies of the combination of time-dependence and coupling to Bosonic baths to MZMs[25,29] seem to suggest powerlaw scaling errors even for keyboard-like braiding schemes.

Our work focuses on the question of diabatic errors in nominally the simplest braiding protocol in a Y-junction type Majorana architecture[1–3] that is coupled to a Bosonic bath (see Fig. 1). The braiding protocol is based on the tunneling induced transport of MZMs[19] where the splitting between pairs of MZMs is used to exchange the decoupled MZMs $\gamma_{y,z}$ (see Fig. 1) that are used to store quantum information. Such a minimal model[1–3] has been previously used in the literature to study the effect of Bosonic bath on diabatic braiding such as in Ref.[23]. This model focuses on the low energy subspace of Majoranas within the larger microscopic system whenever $1/T$ (T being the character-

istic braiding time) is much larger than the energy of quasiparticle excitations that leave the low energy subspace. In this case, the excitation of quasiparticles outside the space of the minimal model is expected to be negligible. Fig. 1 describes a particular example of a braiding protocol that leads to exchange of γ_y and γ_z. Since the system is isolated (apart from coupling to the Bosonic bath) the total Fermion parity of the system is conserved throughout the braiding protocol. Using the fact that at least one of the MZMs $\gamma_{x,y,z}$ are isolated from the rest of the MZMs at any time in the protocol, it can be shown[1] that the two Fermion parity states remain topologically degenerate. Both the initial and final state leave $\gamma_{y,z}$ decoupled from everything else. Therefore, the conservation of Fermion parity equates the conservation of the MZM parity $i\gamma_y\gamma_z$, which is used to store quantum information, to the conservation of the of the Fermion parity of the coupled pair $\gamma_{0,x}$. The latter is associated with excitations of the system, so that the bit-flip error is directly related to the rate of exciting the system out of the ground state into the excited state. The ground and excited states are the only states in a fixed Fermion parity sector, so that the problem of determining the bit-flip error maps to the excitation probability of spin in a time-dependent magnetic field. Later we will show that the system in Fig. 1 is topologically protected against dephasing errors in the Fermion parity basis. Therefore the problem of bit-flip errors in the system in Fig. 1 can be mapped entirely to the relatively well-studied problem of diabatic errors for a spin in a time-dependent magnetic field (see for e.g.[30,31]).

Despite the mapping of the system in Fig. 1 to a spin in a magnetic field, the topological nature of the set-up leads to certain unique features when considering interactions of the system with a Bosonic bath. Microscopically we assume that the Bosonic bath enters all the parameters of the semionductor nanowire model[7,8] such as chemical potential. The changes in these parameters lead to variations in the tunnel coupling between the Majoranas. In the spin representation, each of the tunnelings of the MZMs such as $i\gamma_0\gamma_a$ can be viewed as a component B_a of a magnetic field for $a = x, y, z$. Thus, we can model the coupling of the Bosonic bath to the effective spin as a magnetic field noise similar to the classic spin-Boson model[32,33]. To simplify our treatment, we assume that the coupling to the Bosonic bath is weak compared to temperature (much smaller than the gap) so that the bath can be modeled within the Markovian approximation using the Davies prescription [34,35]. However, unlike a conventional spin, the vanishing of a component of the magnetic field also implies a vanishing of the noise. This is because such a vanishing of a component of the magnetic field is assumed to occur because of isolation of one of the MZMs from the rest of the system. This leads to conservation of the associated MZM operator, which in turn leads to conservation of the associated excitation. Specifically, this means that for the setup in Fig. 1, the Bosonic bath is forced to decouple from the topologically protected quantum information at the end of the process. However, this also means that any excitation generated during the dynamics of the effective magnetic field cannot relax away at the end of the process. This is in contrast to the dynamics in the spin-Boson model, where the system in contact with a zero-temperature Bosonic bath would always relax back to the ground state once the magnetic field becomes static at the end of the process. The absence of such relaxation leads to the a finite excitation probability in the braiding set-up in Fig. 1, which leads to the possibility of the bit-flip error studied in this work.

Motivated by the mapping of the set-up of Fig. 1 to a spin in a magnetic field, in this work we study the probability of excitation of a spin in a time-dependent magnetic field that is coupled to a Bosonic bath. The coupling to the Bosonic bath is assumed to be small enough so that it can be studied within the Markovian approximation using the Davies prescription [34,35]. This leads to a time-dependent master equation which is further reduced to a Bloch equation describing spin-1/2 particles with relaxation and dephasing[35,36]. To simplify the parameter space of possibilities, we assume that the temperature is low enough so that thermal excitation can be ignored. In absence of such induced thermal excitations, the bath decoheres the effective spin-1/2 system through two mechanisms, namely, dephasing, which scrambles the relative phase between the ground and the excited state of the spin-1/2 system without imparting/removing energy to/from the system and relaxation, which induces the system in the excited state to relax back to the ground state. For an isolated system (absence of system-bath coupling), the scaling of diabatic error (which is a measure of the excitation probability in such a spin-system) with respect to the braiding time T, is sensitive to the smoothness of the diabatic drive[37–39] where, in the limit of perfectly smooth (analytic C^∞) drive, the diabatic error is exponentially suppressed[40–42] as opposed to polynomial scaling of the diabatic error found when the drive is not perfectly smooth (for e.g. when the n^{th} time-derivative is discontinuous at the turning points of the drive, which occur when the vector representing Majorana coupling is directed entirely along X,Y or Z axis in Fig. 1).

In present paper thus, we work in the limit of perfectly smooth diabatic drive. Using arguments similar to the ones developed in Ref.[42], we analytically rederive an established result of Ref.[42] that shows the error in diabatic braiding scales exponentially in braiding time T for an isolated system. We augment this known result, by providing strong numerical evidence that the precise exponential dependence on T scales as $e^{-\sqrt{T}}$. The analytic method hence developed generalizes to the case of Bosonic bath interacting with the Majorana system. It is immediately found that in the special case where no relaxation mechanism is present, finite dephasing leads to a diabatic error that scales polynomially as T^{-1} in braiding time, T. Furthermore, we show that by introducing bath-induced relaxation, the diabatic error scaling is slightly improved to T^{-2}. Our result compliments and is consistent with the numerical evidence and heuristic arguments put forth in Ref.[23] where the same, T^{-2} power-law scaling of the diabatic error in presence of a Bosonic bath (see Fig. 2,3 in Ref.[23]) was suggested.

The rest of the paper is organized as follows. In Sec.II, we map the time dependent braiding Hamiltonian describing Fig. 1 to an effective two-level spin-1/2 system coupled to a bath described by a Bloch equation. In Sec.III, following the analytical method developed in Ref.[42], we introduce the framework to calculate diabatic corrections to the time-evolved ground-state and study diabatic corrections in the absence of bath coupling and present an analytical formula to calculate diabatic correction for a purely dephasing bath (i.e. in presence of bath-induced dephasing but complete absence of absence of relaxation). In Sec.IV we study our system coupled to a general bath where both dephasing and relaxation mechanisms are present. We summarize our re-

sults in Sec.V and provide details of our calculations in the appendix.

II. BRAIDING HAMILTONIAN AND BOSONIC BATH

In this section, we setup the description of the Majorana system coupled to the bath as a Master equation that describes the effect of the bath on the time-evolution of the density matrix through a sequence of so-called *jump* operators[36]. Below we first show how the Majorana braiding system shown in Fig. 1 can be described by an effective spin-1/2 Hamiltonian in a fixed Fermion parity sector[23]. We then write down the jump operators in the Master equation that describe the coupling to the thermal bath. Finally we recast the Master equation in the Lindblad form into a Bloch equation.

A. Spin-$1/2$ representation of braiding Hamiltonian

The ideal system (i.e. apart from the bath) comprise four Majoranas labeled $\gamma_0, \gamma_x, \gamma_y, \gamma_z$ shown in Fig. 1. The unitary time evolution generated by the time-dependent braiding Hamiltonian over a time cycle results in exchange of two specific Majoranas. Such a braiding Hamiltonian is given by

$$H = i\gamma_0(\vec{B}(t).\vec{\gamma}), \tag{1}$$

with $\vec{\gamma} = (\gamma_x, \gamma_y, \gamma_z)$. The Hamiltonian H of the system coupled to the bath conserves Fermion parity $P = \gamma_0\gamma_x\gamma_y\gamma_z$. We use the lowest energy state of each parity $P = \pm 1$ to define the qubit. Choosing $\vec{B}$ describes coupling among Majoranas such that there is atleast one uncoupled Majorana γ_i for $i \in \{x, y, z\}$ at any time ensures a topological degeneracy[1]. To understand this, we label the Majorana γ_i as the isolated Majorana at a particular time and check that

$$[P, H] = [\gamma_i, H] = \{P, \gamma_i\} = 0. \tag{2}$$

If we define $|\psi_{P=1}(t)\rangle$ as the instantaneous ground state with even parity $P = 1$, it follows from Eq. 2 that the $|\psi_{P=-1}(t)\rangle = \gamma_i|\psi_{P=1}(t)\rangle$ is an eigenstate of H, which is degenerate with $|\psi_{P=1}(t)\rangle$ and has odd Fermion parity (i.e. $P = -1$).

Now we show that the Hamiltonian described in Eq. 1, that time-evolves as described in Fig. 1 executes an exchange of two Majoranas if the system is somehow found in its ground state at the three turning points (which occur when $\vec{B}$ points entirely along X, Y or X axis as described in Fig. 1). Clearly, this condition is satisfied if the time-evolution is infinitely slow (i.e. adiabatic). However, other approaches such as adding a counterdiabatic term to the Hamiltonian may allow to bypass the infinitely-slow-time-evolution criterion[43]. Regardless, we will assume that the system is in the ground state at the turning points of the braid for the sake of this argument but drop this assumption beyond this subsection for the rest of the paper. The time evolution of the Majoranas is governed by the Hamiltonian H where the time-dependent magnetic field $\vec{B}(t)$ shows a three step time dependence shown in Fig. 2. These steps are defined by the vanishing of one of the components B_z, B_x and B_y, respectively, which implies the isolation of the corresponding Majorana $\gamma_{i=x,y,z}$ that is required to guarantee the topological degeneracy. Using the relations Eq. 2, we can use the isolation of γ_z (i.e. $[\gamma_z, H] = 0$) at time $t = 0$, to constrain the time-evolution of a pair of states related by:

$$|\Psi_{P=-1}(t)\rangle = \gamma_z|\Psi_{P=1}(t)\rangle \tag{3}$$

at time $t = 0$. Eq. 2 lets us extend this relation from $t = 0$ to the entire first segment $0 < t < T$.

We can extend the above relationship between the ground states in the two parity sectors through rest of the braid if we assume that the system is in the ground state at the turning points. Using this assumption at time $t = T$, where (γ_y, γ_0) are the only coupled Majoranas, the parity of the gapped wires maybe constrained as

$$i\gamma_0\gamma_y|\Psi_{P=1}(t = T)\rangle = -|\Psi_{P=1}(t = T)\rangle. \tag{4}$$

Since $P = \gamma_0\gamma_x\gamma_y\gamma_z$, this also implies

$$|\Psi_{P=-1}(T)\rangle = \gamma_z|\Psi_{P=1}(T)\rangle = i\gamma_x|\Psi_{P=1}(T)\rangle. \tag{5}$$

Repeating the arguments from Eq. 3,4,5 two more times leads to the relation

$$|\Psi_{P=-1}(t)\rangle = i\gamma_z|\Psi_{P=1}(t)\rangle \tag{6}$$

at $t = 3T$. Comparing this equation to Eq. 3, we realize that within the low-energy subspace spanned by $|\Psi_{P=\pm1}\rangle$, the unitary time-evolution (ignoring an overall phase) can be written as $U = e^{\pi\gamma_z\gamma_y/4}$, which is the standard representation[4] for exchanging the Majoranas $\gamma_{z,y}$. Note that the only assumption that was crucial for this argument was that the Majorana part of the system remains in the ground state at the turning points during the time evolution. In principle, this allows us to consider $|\Psi_P(t)\rangle$ to be a wave-function of a Majorana system interacting with a Bosonic bath that we will consider later. Therefore, we can conclude that the qubit error (both bit-flip and dephasing) probability for the set-up in Fig. 1 is given by the probability of excitation of the system out of the ground state in a fixed parity sector calculated at the turning point.

The flexibility of being able to focus on the excitation probability in a fixed parity sector allows us to map the Majorana dynamics problem to that of a spin-$1/2$ system. To see this we note that the Majorana operators may be expressed in terms of Pauli matrices as:

$$\begin{aligned} \gamma_x = \sigma_x\tau_x \quad ; \quad \gamma_y = \sigma_y\tau_x \\ \gamma_z = \sigma_z\tau_x \quad ; \quad \gamma_0 = \tau_y, \end{aligned} \tag{7}$$

(where τ and σ are two sets of Pauli matrices) so that Eq. 1 can be rewritten as,

$$H = \vec{B}(t).\vec{\sigma}\tau_z. \tag{8}$$

The Hamiltonian commutes (i.e. $[H, \hat{P}] = 0$) with the fermionic parity operator $\hat{P} = \gamma_0\gamma_x\gamma_y\gamma_z = \tau_z$. Within the $P = \tau_z = 1$ parity sector, the dynamics of the system may be described by the reduced *2-level* Hamiltonian,

$$H_{2Level} = \vec{B}(t).\vec{\sigma}. \tag{9}$$

Derivative discontinuities in the time-dependence of $\vec{B}(t)$ are known to introduce diabatic errors in Majorana

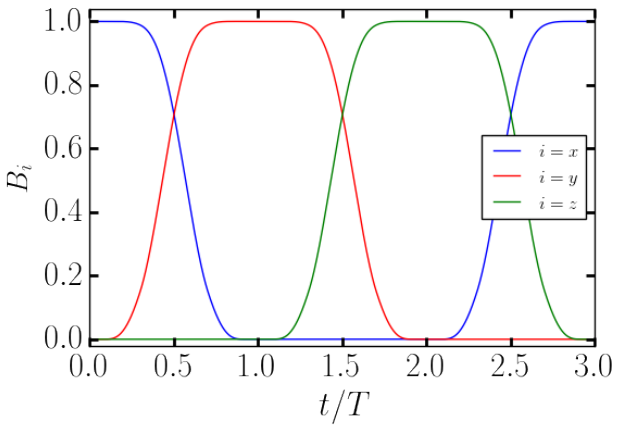

FIG. 2: Plot of different components of Majorana coupling field (B_i ; $i \in \{x, y, z\}$) appearing in Eq. 1 as a function of scaled-time for $s = t/T$ as described by Eq. 10

qubits that scale as a power-law in T[23]. To avoid such diabatic errors the profile for $\vec{B}(t)$ in Fig. 2 is chosen to be a piece-wise continuous functions where all derivatives are continuous (i.e. C^∞). The specific form in Fig. 2 that accomplishes this level of smoothness is given by

$$B_x = \begin{cases} \cos(\theta(s)), & 0 \le s < 1 \\ 0, & 1 \le s < 2 \\ \sin(\theta(s-2)), & 2 \le s \le 3 \end{cases}$$
$$B_y = \begin{cases} \sin(\theta(s)), & 0 \le s < 1 \\ \cos(\theta(s-1)), & 1 \le s < 2 \\ 0, & 2 \le s \le 3 \end{cases}$$
$$B_z = \begin{cases} 0, & 0 \le s < 1 \\ \sin(\theta(s-1)), & 1 \le s < 2 \\ \cos(\theta(s-2)), & 2 \le s \le 3. \end{cases} \quad (10)$$

where

$$\theta(s) = \frac{\pi \int_0^s ds' e^{-1/s'(1-s')}}{2\int_0^1 ds' e^{-1/s'(1-s')}}, \quad s \in [0,1] \quad (11)$$

and

$$s \equiv t/T. \quad (12)$$

is the dimensionless time parameter.

B. Master Equation

Here we describe the Master equation that we use to model the interaction of the system with a parity-conserving thermal bath within the Born-Markov approximation. As discussed such a bath can only generate errors by flipping the system to the excited state of the spin Hamiltonian H_{2level} in Eq. 9. Therefore, similar to the previous subsection, it suffices us to derive a Master equation for the spin-1/2 system[23].

The total Hamiltonian describing the system interacting with a bosonic bath is,

$$H_T = H_{2level} + H_{SB} + H_B, \quad (13)$$

where, H_{2level}, H_B, H_{SB} are system Hamiltonian, bosonic-bath Hamiltonian and Hamiltonian describing system-bath coupling, respectively. In general, the system-bath Hamiltonian have the following form,

$$H_{SB} = \sum_k \hat{A}_k \hat{\Gamma}_k, \quad (14)$$

where $\hat{A}_k$ and $\hat{\Gamma}_k$ are system and bath operators, respectively, satisfying $\hat{A}_k^\dagger = \hat{A}_k$ and $\hat{\Gamma}_k^\dagger = \hat{\Gamma}_k$.

Following the prescription introduced by Davies[34], under the assumptions of weak system-bath coupling (*Born* approximation) and memory-less bath (*Markov* approximation: bath correlation time vanishes on system time scales), the master equation describing the time evolution of density matrix of the system can be expressed in the *Lindblad* form[34,35] as

$$\dot{\rho}_S(t) = -i[H_{2level}, \rho_S(t)] + \mathcal{D}(\rho_S(t)), \quad (15)$$

where the bath term is written as:

$$\mathcal{D}(\rho_S(t)) = \sum_{\nu,k} J_k^\nu(t)\rho_S(t)J_k^{\nu\dagger}(t)\eta_k(\nu) - \frac{1}{2}\eta_k(\nu)\{J_k^\nu(t)^\dagger J_k^\nu(t), \rho_S(t)\}. \quad (16)$$

The above bath-induced dissipation term is written in terms of projections $J_k^\nu(t)$ of the system operators $\hat{A}_k(t)$, referred to as "jump operators" that are written as

$$J_k^\nu(t) = \sum_{e'-e=\nu} \Pi(e)\hat{A}_k(t)\Pi(e'), \quad (17)$$

with $\Pi(e)$ being the projection operator to an eigenspace spanned by eigenstates of H_{2level} with eigenvalue e. The coefficients $\eta_k(\nu)$ in Eq. 16 are correlators of the bath operators that are written as

$$\eta_k(\nu) = \mathrm{Re}\int_{-\infty}^{\infty} ds e^{-i\nu s}\left\langle \hat{\Gamma}_k^\dagger(s)\hat{\Gamma}_k(0)\right\rangle \quad (18)$$

where, $\langle\cdots\rangle$ denotes thermal average, $\mathrm{tr}_B(\cdots\rho_B)$. Depending on the value of ν, the jump operators J_k^ν are classified as excitations ($\nu > 0$), relaxation ($\nu < 0$) or dephasing ($\nu = 0$).

The bath operators couple to each of the components of B_i (where $i = \{x, y, z\}$) in a way where the bath coupling to a particular wire in Fig. 1 vanishes when the corresponding B_i vanishes. This is essential to represent the fact that the vanishing B_i results from decoupling of γ_i from γ_0. To satisfy this condition, we choose the system operators for the bath coupling as

$$\hat{A}_i = s_i B_i \sigma_i. \quad (19)$$

Using Eq. 17, the *jump operators* corresponding to the above choice of $\hat{A}$ operators are expressed as,

$$J_i^\nu(t) = s_i a_i(t) B_i(t)|1(t)\rangle\langle 0(t)|; \quad J_i^{-\nu} = J_i^{\nu\dagger}$$
$$J_i^{\nu=0} = s_i B_i(t)(a_i^0(t)|0(t)\rangle\langle 0(t)| + a_i^1(t)|1(t)\rangle\langle 1(t)|) \quad (20)$$

where,

$$a_i(t) = \langle 1(t)|\sigma_i|0(t)\rangle$$
$$a_i^0(t) = \langle 0(t)|\sigma_i|0(t)\rangle$$
$$a_i^1(t) = \langle 1(t)|\sigma_i|1(t)\rangle, \quad (21)$$

s_i being the time-independent system-bath coupling strength with $i \in \{x, y, z\}$ and $|0(t)\rangle$ and $|1(t)\rangle$ denoting the instantaneous ground and the excited states of $H_{2level}(t)$, respectively.

We wish to focus on only those bath-effects that arise due to time-dependence of the Hamiltonian. In other words we want to explicitly avoid any bath-induced effect that do not vanish in the adiabatic limit provided the system is initialized in the ground state. The only such environmental effect is thermal excitation associated with $J^{\nu=2}$ (energy gap above ground state is 2 for $\|\vec{B}\| = 1$) operator. We explicitly set temperature to zero to completely suppress these thermal excitations or equivalently,

$$\eta(\nu = 2) = 0. \tag{22}$$

Since the braiding process involves sequence of three identical clockwise $\pi/2$ rotations of $\vec{B}$ along $\hat{z}, \hat{x}$ and $\hat{y}$ axes respectively, as shown in Fig. 1, we focus on the first sequence where $\vec{B}$ is restricted to XY plane without loss of generality, setting $B_z = 0$. Influence of the bath is captured by the strength of the system-bath couplings (captured by s_x and s_y), the relaxation strength governed by $\eta(\nu = -2)$ (since the gap in the system is 2) and dephasing strength governed by $\eta(\nu = 0)$. Since the time-dependence of the Hamiltonian does not affect the gap in the system $\eta(\nu = -2)$ and $\eta(\nu = 0)$ are fixed parameters determined by entirely by the microscopic properties of the bath Hamiltonian. From here onwards, for the sake of brevity, we relabel the relaxation strength, $\eta(\nu = -2)$ and the dephasing strength, $\eta(\nu = 0)$ with new symbols, $\eta(\nu = -2) \equiv \eta$ and $\eta(\nu = 0) \equiv \eta_0$.

C. Bloch equation

The density matrix $\rho_S(t)$ appearing in the master equation (Eq. 15 can be parametrized in terms of a Bloch vector $R \equiv (r_x, r_y, r_z)$ defined by

$$\rho_S(t) = \frac{1}{2}(r_x(t)\sigma_x + r_y(t)\sigma_y + r_z(t)\sigma_z + \mathbb{1}). \tag{23}$$

Rewriting the Master equation (Eq. 15) in terms of $\vec{R}$ leads to the so-called Bloch equation

$$\epsilon\dot{\vec{R}} = 2[\vec{B} \times \vec{R} + (\alpha - \beta)\vec{B} \times (\vec{B} \times \vec{R}) - 2\beta(\vec{B} + \vec{R})] \tag{24}$$

where,

$$\begin{aligned} \beta(s) &= \frac{1}{4}F(s)\eta; \quad \text{(effective relaxation)} \\ \alpha(s) &= F^0(s)\eta_0; \quad \text{(effective dephasing)} \end{aligned} \tag{25}$$

with,

$$\begin{aligned} F &= s_x^2 B_y^2(s) B_x^2(s) + s_y^2 B_x^2(s) B_y^2(s) \\ F^0 &= s_x^2 B_x^4(s) + s_y^2 B_y^4(s) \end{aligned} \tag{26}$$

and $\epsilon = 1/T$. Note that the time derivatives in the above equation refer to the rescaled time $s = t/T$.

The Bloch equation can be more compactly expressed in a matrix form as,

$$\epsilon\frac{d}{ds}R = MR + 4\beta(R_0 - R) \tag{27}$$

with, $R_0(s) \equiv -\vec{B}(s)$ being a null vector of M, $M = 2(A + S)$ and $S = (\alpha - \beta)A^2$ where,

$$A = \begin{pmatrix} 0 & 0 & B_y \\ 0 & 0 & -B_x \\ -B_y & B_x & 0 \end{pmatrix} \tag{28}$$

III. ADIABATIC EXPANSION FOR BLOCH EQUATION

As discussed in Sec. I, the diabatic error for the Majorana qubit in Fig. 1 is related to the probability of transition out of the ground state. Such a transition can occur in any one of the three steps of the braiding protocol, so that the order of magnitude of the error can be estimated from the transition probability in any one step. We consider the first step of the braiding process where $B_z = 0$ and calculate the diabatic error incurred in the process which involves rotating $\vec{B}$ along $\hat{z}$ axis by $\pi/2$ in the clockwise direction from the initial orientation along $\hat{x}$ to final orientation along $\hat{y}$. The system is initialized in the ground state of H_{2Level} to which the corresponding Bloch vector is $R(s = 0) = -\vec{B}(s = 0) = (-1, 0, 0)$. Given this initial condition, the solution of the Bloch equation (i.e. Eq. 27) in the extreme adiabatic limit (i.e. $\epsilon = 0$), is written as:

$$R(s) = R_0(s). \tag{29}$$

At non-zero ϵ, the time-dependent solution $R(s)$ of the Bloch equation 27, referred to as *time-evolved Bloch zero-vector* (TBZV), differs from the adiabatic limit $R_0(s)$. The magnitude of the difference at $s = 1$

$$\mathcal{E} \equiv \|R(1) - R_0(1)\|, \tag{30}$$

quantifies the diabatic error for the braiding.

Let us now consider the solution of the Bloch equation Eq. 27 for infinitesimal ϵ. We first focus on the case of vanishing relaxation (i.e. $\eta = \beta = 0$) where the Bloch equation reduces to

$$\epsilon\dot{R} = MR. \tag{31}$$

The finite relaxation situation will be dealt with in Sec. IV using a slightly different technique. The solution of the Bloch equation in the above form admits an adiabatic series expansion written as:

$$R(s) = R_0(s) + \epsilon R_1(s) + \epsilon^2 R_2(s) \ldots \tag{32}$$

Substituting the above ansatz in Eq. 31 and equating both sides of the equation at each order in ϵ we formally solve for j^{th} order correction to $R_0(s)$ for $R(s)$ (see App. A for details),

$$R_j = f_{j-1}R_0 + M^{-1}\dot{R}_{j-1} \tag{33}$$

with $f_{j-1}(s)$ given by,

$$f_{j-1}(s) = \int_0^s ds\, \dot{R}_0^T M^{-1} \dot{R}_{j-1}. \tag{34}$$

The matrix M is singular so that it is crucial to note that Eq. 31 implies that $R_0^T \dot{R} \propto R_0^T M R = 0$. Additionally this implies that the generalized inverse M^{-1} can be defined so that $M^{-1}\dot{R}$ is orthogonal to $R_0(s)$. Motivated by this, it is convenient to split the expansion (Eq. 32) into two parts

$$R(s) = f(s)R_0(s) + R_\perp(s) \tag{35}$$

where, $R_0^T(s)R_\perp(s) = 0$ and $f(s)$ and $R_\perp(s)$ are expanded as:

$$\begin{aligned} f(s) &= 1 + \epsilon f_0(s) + \epsilon^2 f_1(s) + \dots \\ R_\perp(s) &= M^{-1}(\epsilon \dot{R}_0(s) + \epsilon^2 \dot{R}_1(s) + \dots). \end{aligned} \tag{36}$$

Taking repeated derivatives of Eq. 33(see App. A for details) we can show that $\dot{R}_j(s=1)$ vanishes when all derivatives of R_0 vanish, $R_0^{(n)}(s) \equiv -\vec{B}^{(n)}(s) = 0$ at $s = 0, 1$. This implies that $R_\perp(s=1)$ vanishes as well only when the magnetic field $\vec{B}(s)$ goes to 0 smoothly at $s = 0, 1$, which is a condition that is ensured by the specific time-dependence of the magnetic field chosen (i.e. Eq. 10). More precisely, considering the expansion for $R_\perp$ (Eq. 36) to a finite order n, one can show that

$$\|R_\perp(s=1)\|/\epsilon^n = 0 \; as \; \epsilon \to 0 \tag{37}$$

for every integer n. This shows that $R_\perp(s=1)$ vanishes faster than any power-law in the adiabatic limit. A numerical analysis shows that

$$\|R_\perp(s=1)\| \sim e^{-\sqrt{T}}, \tag{38}$$

which is similar to (but slower than) exponential scaling with T.

In the absence of any bath (i.e. $\eta = \eta_0 = \alpha = \beta = 0$) the dynamics of $R(s)$ is unitary and $\|R(s)\| = 1$. Thus the bound on $R_\perp(s=1)$ (Eq. 38) also implies a bound on the diabatic error for the isolated qubit given by

$$\mathcal{E} = \|R(1) - R_0(1)\| \sim e^{-\sqrt{T}}. \tag{39}$$

This is completely consistent with the numerical results in Fig. 3 and also with those derived in Ref.[42], which suggests an exponential-like dependence of diabatic error $\mathcal{E}$ on T. Note that such exponential scaling follows entirely from the unitarity of time evolution and Eq. 38. However, it is clear from the defining equation for $R_\perp$ in Eq. 36 and the mathematical relations in Eqs. 32-35 that the diabatic drive (equivalently M in Eq. 31) must be an analytic function (i.e. C^∞) of time. The result in Eq. 39 does not hold if the diabatic drive is non-analytic as shown in Ref.[23]. In that work, the authors consider non-analytic diabatic drives with varying smoothness (i.e. diabatic drives that are C^k for varying values of k) and find k-dependent polynomial scaling for asymptotic diabatic error (see Fig. 2,3 in Ref.[23]).

In the presence of dephasing $\eta \neq 0$, the unitarity constraint $\|R(1)\| = \|R_0(1)\|$ does not apply, but one can use the essential vanishing of $R_\perp(s=1)$ (Eq. 37) in combination with Eq. 35 to write

$$R(1) = f(1)R_0(1). \tag{40}$$

Evaluating the recursive relation Eq. 34, one finds (see App. A for details) a non-vanishing $O(\epsilon)$ contribution to $f(1)$ that is written as

$$f_0(1) = -\int_0^1 \frac{\alpha\omega^2}{2(1+\alpha^2)} ds. \tag{41}$$

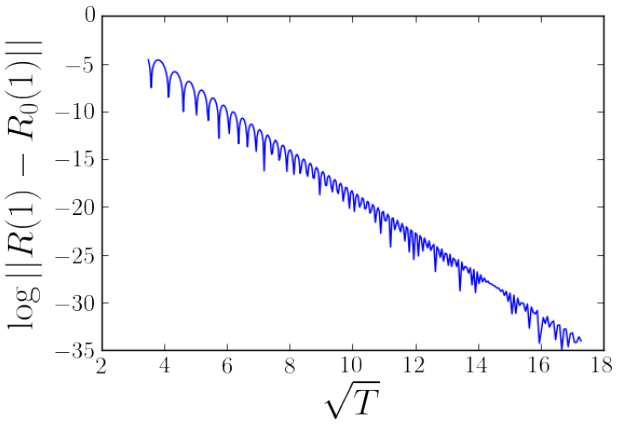

FIG. 3: Numerical plot of log of norm of difference between time evolved and instantaneous Bloch zero-vector at scaled time $s = 1$ as a function of $\sqrt{T}$ for strength $s_x = s_y = 0$ obtained using Eq. 27. The system is initialized in the ground state of H_{2Level} or equivalently the initial value of $R(s=0)$ in the Bloch equation is set as $R_0(0) = -\vec{B}(0)$. The plot shows exponential decay in $\mathcal{E}$ as a function of total time T when system-bath coupling is zero consistent with the result derived in App. A. Specifically, $\mathcal{E} = \|R(1) - R_0(1)\| \sim e^{-\sqrt{T}}$.

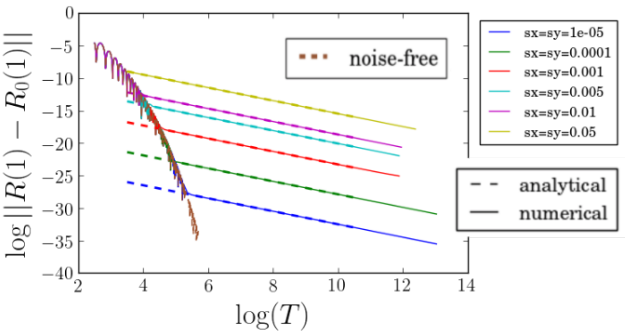

FIG. 4: Plot of $\mathcal{E}$ as a function of time T for different values of effective dephasing strength α characterized by values of $s_x = s_y$ and absence of effective relaxation, $\beta = 0$ (see Eq. 25). Relaxation and dephasing parameters, η and η_0, that solely depend on bath Hamiltonian are set to $\eta = 0$ and $\eta_0 = 1$, respectively. The solid line is obtained by solving the Bloch equation (Eq. 31) and is compared against (dashed curve) theoretical bound given by Eq. 42,41, i.e., dashed curve is calculated value of $\log[(1/T)f_0(1)]$ using the expression given in Eq. 41. The low-T region characterized by the oscillatory section of the curves are independent of system-bath coupling strength and follows closely the numerical values obtained by solving the Bloch equation (Eq. 27) in absence of bath denoted by the dashed-brown-colored curve.

This leads to a power-law diabatic error estimate,

$$\mathcal{E} = \|R_0(1)\|\big|(1 - f(1))\big| \approx -\epsilon f_0(1) \tag{42}$$

Note that such error term (as well as the other powers of ϵ) dominate over $e^{-\sqrt{T}}$ estimate for the $R_\perp(s=1)$ component that was ignored but would vanish in the absence of a bath ($\alpha = 0$) restoring the exponential estimate for the isolated system situation.

In Fig. 4, we plot $\log\mathcal{E}$ as a function of $\log(T)$ for different system-bath coupling strengths and compare it against numerical curve obtained by solving Eq. 31. We find that numerically exact calculation of $\mathcal{E}$ validates the asymptotic

(large T) limit of the diabatic error (Eq. 42) obtained for truncation at first-order in epsilon. We find that the scaling region that follows Eq. 42 begins rather abruptly above a value of T that depends on the dissipation strength. The behavior below this threshold coincides with the behavior of the dissipationless system shown in Fig. 3. Thus, the strength of the dissipation determines the critical braiding rate above which the exponential behavior of diabatic error (Eq. 39) crosses over into power-law error described by Eq. 42.

IV. GENERAL SYSTEM-BATH COUPLING

We now consider the error $\mathcal{E}$ in the presence of finite relaxation. In order to solve for R in Eq. 24 for the case of finite β we switch to a new vector-variable $\vec{\Pi}$,

$$R(s) = U_0(s)(-\hat{x} + \vec{\Pi}(s)) \tag{43}$$

where, $U_0(s)$ is the rotation matrix such that $R_0(s) = U_0 R_0(0)$ ($R_0(0) = -\hat{x}$ being the initial condition on R) given by

$$U_0 = \begin{pmatrix} \cos\theta & \sin\theta & 0 \\ -\sin\theta & \cos\theta & 0 \\ 0 & 0 & 1 \end{pmatrix}. \tag{44}$$

From Eq. 43 it follows, the initial condition on $\Pi(s)$ is $\Pi(0) = (0,0,0)$. Since $R_0(s)$ is the solution to the Bloch equation in $\epsilon \to 0$ limit, $\Pi(s)$ must have perturbatively small norm in ϵ.

The equation of motion for $\Pi(s)$ is found to be,

$$\epsilon\left(\dot{\vec{\Pi}} + \dot{\theta}\hat{z}\times\vec{\Pi} - \dot{\theta}\hat{y}\right) = 2\hat{x}\times\vec{\Pi} + 2(\alpha-\beta)\hat{x}\times(\hat{x}\times\vec{\Pi}) - 4\beta\vec{\Pi}. \tag{45}$$

On the right hand side of the equation, the operator acting on Π can be diagonalized along the basis unit vectors $\{\hat{x}, \hat{j}_+, \hat{j}_-\}$ with $\{-4\beta, 2\lambda_+, 2\lambda_-\}$ being the corresponding eigenvalues where we have defined,

$$\hat{j}_\pm = \frac{1}{\sqrt{2}}(\hat{y} \pm i\hat{z}) \tag{46}$$

$$\lambda_\pm = \mp i - (\alpha+\beta). \tag{47}$$

Representing $\vec{\Pi}$ in this basis set,

$$\vec{\Pi} = \pi_x\hat{x} + \pi_+\hat{j}_+ + \pi_-\hat{j}_- \tag{48}$$

leads to the following coupled-differential-equation,

$$\epsilon\left[\dot{\pi}_x - \frac{\dot{\theta}}{\sqrt{2}}(\pi_+ + \pi_-)\right] = -4\beta\pi_x \tag{49a}$$

$$\epsilon\left[\dot{\pi}_\pm + \frac{\dot{\theta}}{\sqrt{2}}\pi_x - \frac{\dot{\theta}}{\sqrt{2}}\right] = 2\lambda_\pm\pi_\pm \tag{49b}$$

Finite relaxation $\beta > 0$ ensures that at sufficiently long time T (or sufficiently small ϵ), the memory of the initial conditions at $s = 0$ are exponentially suppressed. In this case, Eq. 49a suggests $\pi_x(0 < s < 1)$ is $O(\epsilon)$ so that, to lowest order in ϵ,

$$\pi_\pm \approx -\frac{\dot{\theta}\epsilon}{\sqrt{2}\lambda_\pm}. \tag{50}$$

This implies $\pi_+(1) = \pi_-(1) \approx 0$ as $\dot{\theta}|_{s=1} = 0$ (see Eq. 11). Therefore, we conclude $\mathcal{E} = \|R(1) - R_0(1)\| \approx \pi_x(1)$. Substituting $\pi_\pm$ expressions in Eq. 49a, it can be solved for π_x resulting in

$$\mathcal{E} \simeq \pi_x(1) = -\epsilon\int_0^1 \dot{f}_0 e^{-\frac{4}{\epsilon}\int_s^1 \beta ds'} ds. \tag{51}$$

where we have defined,

$$f_0(s) = -\int_0^s \frac{(\alpha+\beta)\dot{\theta}^2}{2(1+(\alpha+\beta)^2)} ds'. \tag{52}$$

In the above expression the integral is performed over the scaled time parameter s' which explicitly governs α, β and θ. The behavior of $\mathcal{E}$ in the large-T limit is analyzed using saddle-point method detailed in the App. B to obtain the following asymptotic form for the diabatic error,

$$\mathcal{E} \sim e^4 T^{-2}. \tag{53}$$

Note that Eq. 51 reduces to Eq. 42 in absence of relaxation, i.e. $\beta \to 0$, showing that the approach in this section is not inconsistent with that in the previous section for the case without relaxation. An examination of the exponential factor in Eq. 51 tells us that for the case where relaxation is weak compared to dissipation (i.e. $\beta \lesssim \alpha$), we should expect an intermediate regime of ϵ where β might still be ignored so that the error would scale as $\mathcal{E}(T) \sim T$ as concluded in the previous section.

Therefore as T is increased we expect the error rate $\mathcal{E}$ to crossover from the isolated system limit (Eq. 39) to the dominantly dissipative system(Eq. 42) to the asymptotics with relaxation (Eq. 53). The numerical plot of the error rate $\mathcal{E}$ in the general case, Fig. 5 indeed shows this expected pattern of crossovers. These expectations turn out to be quite accurate as seen from the numerical simulations in Fig. 5, which shows the numerical estimate of $\mathcal{E}$ vs total time T in log-log scale for dephasing strength η_0, and relaxation strength η, both set equal to 1. It is interesting that the crossover behavior expected for the limit $\eta_0 \gg \eta$ seems to apply even to $\eta_0 = \eta = 1$ chosen for Fig. 5. Finally, we see in Fig. 5 that as we decrease the bath coupling strength $s_x \sim s_y$, the crossover scale modes to higher T as expected. While Eq. 52 predicts the correct crossover behavior, it turns out to be off by a T-independent scale factor in the pre-asymptotic dissipation dominated regime. We have remedied this by adapting the analysis in Sec. III to finite (but small η) as described in App. B. This analysis leads to a somewhat different approximation for $f_0(s)$ which is written as

$$f_0(s) = -\int_0^s \frac{(\alpha-\beta)\dot{\theta}^2}{2(1+(\alpha-\beta)^2)} ds'. \tag{54}$$

This more exact theoretical form, which is the analytic approximation used in the dashed lines in Fig. 5, can be seen from the figure to fit the numerical results very well in both the dissipative and relaxation dominated regimes. It must

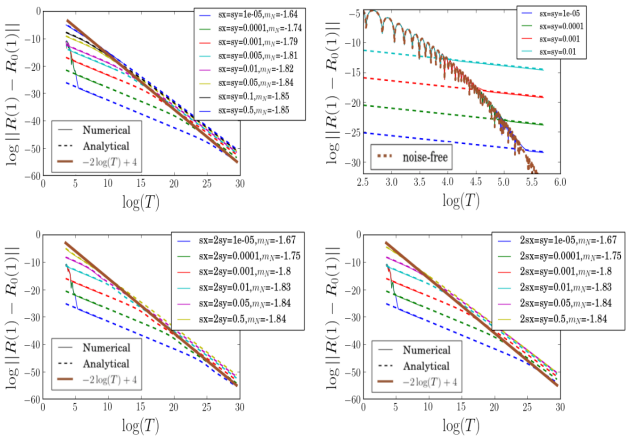

FIG. 5: (Top left) Plot of $\mathcal{E}$ as a function of total-time taken by the diabatic drive T for different values of effective dephasing, α and relaxation strength, β characterized by the shown values of $s_x = s_y$ (see Eq. 27-26). Relaxation and dephasing parameters, η and η_0, that solely depend on bath Hamiltonian are both set to $\eta = \eta_0 = 1$. for all panels in this figure. For each set of parameters, the analytical curve (dashed line) is obtained by plotting the expression in Eq. 51 with f_0 given by Eq. 54. The numerical curve (solid line) is obtained by numerically solving the Bloch equation in Eq. 27. The slope m_N (given in legend) is calculated using the data in the neighborhood of log(T) = 29.5 on the X axis for each curve. The asymptotic dependence on T is given by e^4T^{-2} (Eq. 53), represented in the figure by the solid (thick) brown curve. (Top right) Magnified view of the top left panel in the small-T-region. The values obtained for the special case of zero dephasing and relaxation is plotted using (thick) brown dashed curve. For each coupling strength and sufficiently small values of T, the $\mathcal{E} = \log(R(1) - R_0(1))$ behavior is independent of system bath coupling strength and is well captured by the exponential dependence on T (see Fig.3). The abrupt change from the exponential to a polynomial dependence on T occurs when the analytic estimate of $\mathcal{E}$ coincides with its value under zero system-bath coupling assumption. (Bottom panels) Similar to the top panels, log norm of difference between time evolved and instantaneous Bloch vector at scaled time $s = 1$ ($t/T \mod 3 = 1$)as a function of log of total time T. However, unlike the top panels $s_x = 2s_y$ and $s_y = 2s_x$ for bottom left and right panels respectively. The qualitative behavior is similar to ones observed in the top panels.

be noted that the powerlaw scaling of diabatic braiding in presence of a Bosonic bath with an exponent approximately -2 was found in the numerical investigations carried out in Ref.[23] is consistent with our result in Eq. 53. In that study however, unlike our present work, the diabatic drives for braiding considered are not analytic but instead C^k for some finite k. But the powerlaw exponent was numerically found to be independent of k (see Fig. 2,3 in Ref.[23]), always approximately -2. This is not surprising in the light of discussion in the present and the previous sections where we have argued that in presence of a Bosonic bath (which renders the time-evolution non-unitary) , it suffices to truncate the equation of motion for the Bloch vector to first order in $1/T$ (see Eqs. 42,50). This strongly indicates that in presence of a Bosonic bath, Eq. 53 captures scaling of the diabatic error even for non-analytic diabatic drives, consistent with findings of Ref.[23].

V. SUMMARY

In this work we have studied the diabatic error rate $\mathcal{E}(T)$ as a function of braiding time T (in units of inverse gap) of the Y-junction braiding protocol (shown in Fig. 1) by mapping it to the problem of excitation probability of a spin in a time-dependent magnetic field. Consistent with previous work[42] we find (see Eq. 39) that one can reduce diabatic errors[23] in isolated Majorana systems to be exponentially (scaling as $\mathcal{E}(T) \sim e^{-\sqrt{T}}$) small in the braiding time T (in units of inverse gap) by choosing the time-dependence of the Hamiltonian to be completely smooth (including the beginning and end of the protocol). This analytic result explains the recent observation of exponentially suppressed diabatic errors apparent from numerical simulation of some braiding protocols[24] . In fact, while the requirement of a completely smooth time-dependent Hamiltonian of the form of Eq. 8 (also see Eq. 10) seems fine-tuned, it is quite natural in a topological system where MZM splitting is tuned either by chemical potential[18,24,44] or by screening charging energy through tunable Josephson junctions[3,45]. In both these cases, the tunneling is exponentially suppressed as one tunes the Majorana wire deep into the topological phase or introduces a strong Josephson coupling between the Majorana wire and a bulk superconductor. The main focus of our work is to consider the effect of interaction of the topological system with a Fermion parity conserving Bosonic bath, such as phonons or plasmons on the diabatic error rate for braiding. Similar to previous work[25], we assume the bath to be weakly coupled so that we can treat the bath within the Markovian approximation. We describe the dynamics of this system within the Markovian approximation by a Bloch equation. We find that the coupling to such a Bosonic bath generically changes the asymptotic of the diabatic error from exponential in the braiding time T to power law (i.e. error scaling as $\mathcal{E}(T) \sim e^4T^{-2}$ (see Eq. 53). as expected, the general result including relaxation leads to much lower excited state probability than in the absence of relaxation. We find from a controlled analytic solution that the error rates in the presence of dephasing from the bath but no relaxation decreases the slowest scaling as $\mathcal{E}(T) \sim T^{-1}$.

In addition to the asymptotic forms we study the dependence of the diabatic error rate on the system-bath coupling strength through direct numerical simulations. For purely dephasing bath (i.e. no relaxation), we find (see Fig. 4) that the dephasing strength determines the cross-over from the $e^{-\sqrt{T}}$ scaling error rate that is expected in the absence of a bath to the T^{-1} scaling of the error rate expected for a purely dephasing bath. Increasing the dephasing strength leads to the crossover occuring at shorter braiding time T, in turn leading to error rates that increase with increasing dephasing. As seen from our results in Fig. 5, adding relaxation in addition to dephasing leads to an additional relaxation strength dependent cross-over time-scale beyond which the error rate $\mathcal{E}(T)$ changes its scaling from T^{-1} to $\mathcal{E}(T) \sim e^4T^{-2}$. The reduction of error in the presence of relaxation may be attributed to the decay of some of the excitations back to the ground state from coupling to the bath. Our results assume that the braiding rate is slow compared to the Majorana splitting scale, which in turn is much smaller than the gap to the continuum states. In principle, this can be engineered by carefully chosen Coulomb charg-

ing energy [39,46] that is much smaller than the topological gap. The continuum modes can become important in the case when these conditions are not met. Their effect on our results (particularly the one without relaxation) could be a subject of future inquiry.

In this work, we have ignored finite temperature effects despite the fact that a finite temperature is needed to justify the Markovian approximation. Such finite temperature effects can be expected to be negligible for temperatures substantially below the gap. Moreover, such finite temperature excitations are expected to only increase the excitation probability and thus the error rate. In summary, we find that while a Bosonic bath does not directly interfere with topological protection of quantum information, finite (but low) temperature Bosonic baths can lead to powerlaw in time diabatic errors that might limit the speed of topologically protected operations. However, measurement based error correction schemes might alleviate some of these problems[23].

This work was supported by the Microsoft Station Q, NSF-DMR-1555135 (CAREER), JQI-NSF-PFC (PHY-1430094) and the Sloan research fellowship.

Appendix A: Diabatic expansion of Bloch vector

Expanding the Bloch vector $R(s)$ in powers of $\epsilon = 1/T$,

$$R(s) = R_0(s) + \epsilon R_1(s) + \dots \tag{A1}$$

we seek solution to

$$\epsilon \dot{R} = MR \tag{A2}$$

for initial condiction $R(0) = R_0(0) \equiv \vec{B}(0)$ where, $M = 2(A+S)$ and $S = (\alpha-\beta)A^2$ (A being the matrix representation of $\vec{B}\times$ operation) with α and β being the time-dependent functions defined by Eq. 25. The presentation here follows the work of Hagedorn *et. al.* in Ref.[42].

A, being the anti-symmetric matrix representation of $\vec{B}\times$ operator has eigenvalues $0, i, -i$. Consequently, the instantaneous eigenvalues of M are given by $0, \lambda_1 \text{and} \lambda_2$ with,

$$\begin{aligned}\lambda_1 &= 2(i - (\alpha-\beta))\\ \lambda_2 &= 2(-i - (\alpha-\beta)).\end{aligned} \tag{A3}$$

Denote $R_0(s) = -\vec{B}(s)$ and thereby, $R_0(s)$ is the zero eigenvector with 0 eigenvalue. M can be inverted in the eigenvector subspace with non-zero eigenvalues,

$$M^{-1} = \frac{1}{2(1+(\alpha-\beta)^2)}(-A - (\alpha-\beta)\mathbb{1}). \tag{A4}$$

Expanding $R = R_0 + \epsilon R_1 + \dots$ and substituting in $\epsilon\dot{R} = MR$, we get,

$$\begin{aligned} MR_j &= \dot{R}_{j-1}\\ \implies R_j &= f_{j-1}R_0 + M^{-1}\dot{R}_{j-1}\end{aligned} \tag{A5}$$

with $f_{j-1}(s)$ evaluated using the condition $R_0^{\mathrm{T}}\dot{R}_j = 0$ which follows from $MR_j = \dot{R}_{j-1}$,

$$f_{j-1}(s) = \int_0^s ds\, \dot{R}_0^T M^{-1}\dot{R}_{j-1}. \tag{A6}$$

Now we show that the series expansion is well-defined in small epsilon limit. Consider the partial sum of the series expansion,

$$R^N(s) = \sum_{j=0}^{N} \epsilon^j R_j. \tag{A7}$$

If the series expansion is well-defined, the partial sum (as defined above) must converge to the actual solution R. Let the actual solution $R(s) = V(s)R(0)$. Consider,

$$\begin{aligned}\left\|R^N(s) - R(s)\right\| &= \left\|R^N(s) - V(s)R(0)\right\|\\ &= \|V(s)\|\left\|V(s)^{-1}R^N(s) - R(0)\right\|\\ &= \|V(s)\|\left\|\int_0^s ds' \frac{d}{ds'}V^{-1}(s')R^N(s')\right\|,\end{aligned} \tag{A8}$$

where we have used $\dot{V}^{-1}(0) = 0$ which follows from $\dot{\vec{B}}(0) = 0$. Now,

$$\begin{aligned}\dot{R}^N(s) &= \sum_{j=0}^{N}\epsilon^j\dot{R}_j = \sum_{j=0}^{N}\epsilon^j MR_{j+1}\\ \implies \epsilon\dot{R}^N(s) &= M\sum_{j=0}^{N}\epsilon^{j+1}R_{j+1} + MR_0 - MR_0\\ &= MR^{N+1} = MR^N + \epsilon^{N+1}\dot{R}_N,\end{aligned} \tag{A9}$$

where we simply used the definition given in Eq. A7 and the relation given in Eq. A5 to arrive at the second line above. Using the above relation we get,

$$\frac{d}{ds'}(V^{-1}(s')R^N(s')) = \dot{V}^{-1}R^N + V^{-1}\dot{R}^N = \epsilon^N\dot{R}_N. \tag{A10}$$

Therefore it follows from Eq. A8,

$$\begin{aligned}\left\|R^N(s) - R(s)\right\| &= \|V(s)\|\left\|\int_0^s ds'\epsilon^N\dot{R}_N\right\|\\ &\le \epsilon^N\|V(s)\|\int_0^s ds'\left\|\dot{R}_N\right\|.\end{aligned} \tag{A11}$$

We conclude that R^N converges to the actual solution R provided $\left\|\dot{R}_N\right\|$ and $\|V(s)\|$ are bounded. We refer the reader to Ref.[42] for the proof of boundedness of $\left\|\dot{R}_N\right\|$ in absence of bath. It seems likely that a similar proof holds for boundedness of $\left\|\dot{R}_N\right\|$ in presence of bath. In the limiting $\alpha(s) = \beta(s) = 0$, $V(s)$ is unitary, so clearly when for $\alpha(s) > \beta(s)\forall s$, $\|V(s)\|$ is bounded by 1. Without speculating about $\alpha(s) < \beta(s)$ case, we restrict our following discussion to $\alpha(s) > \beta(s)$ that corresponds to $\eta_0 \ge \eta$ provided $s_x \sim s_y$.

Our goal now is to arrive at a bound for the diabatic error defined by,

$$\mathcal{E} = \|R(1) - R_0(1)\|, \tag{A12}$$

where $R_0(s=1) = -\vec{B}(s=1)$ is the Bloch vector that corresponds to instantaneous zero eigenvector of M at $s =$

1. Note as consistency check that $R(1) \to R_0(1)$ when $\epsilon = 1/T \to 0$ follows from the series expansion of R, Eq. 34. Since we have shown that the series expansion of R is well defined, we can replace R in $\|R(1) - R_0(1)\|$ by its corresponding series expansion. However to make progress towards arriving at a bound for $\mathcal{E}$ we need a useful result stated and proved below.

We show that if all derivative of M (k^{th} derivative denoted by $M^{(k)}$), $M^{(k)}(s_0) = 0 \forall\ k$ for some s_0 then $(R_0^\perp)^T R_j^{(k)} = 0 \forall\ k, j$ where $R_0^\perp$ is any vector such that $(R_0^\perp)^T R_0 = 0$. The proof follows in three steps:

- We first show that $(R_0^\perp)^T R_0^{(k)} = 0 \forall\ k$.
  Let k be a positive integer. $MR_0 = 0 \implies (MR_0)^{(k)} = \sum_{j=0}^{k} \binom{k}{j} M^{(j)} R_0^{(k-j)} = MR_0^{(k)} = 0$.
  Therefore, it must be $(R_0^\perp)^T R_0^{(k)} = 0 \forall\ k$.

- Next we show that $[M^{-1}]^{(k)}(s_0) = 0 \forall\ k$.
  Again, let k be a positive integer. $M^{-1}M = 1 \implies (M^{-1}M)^{(k)} = \sum_{j=0}^{k} \binom{k}{j} [M^{-1}]^{(j)} A^{(k-j)} = [M^{-1}]^{(k)} M = 0$. Therefore, it must be $[M^{-1}]^{(k)}(s_0) = 0 \forall\ k$.

- Finally we prove our original assertion, $(R_0^\perp)^T R_j^{(k)} = 0 \forall\ k, j$.
  We will prove this assertion by induction. Assume $(R_0^\perp)^T R_{j-1}^{(k)} = 0 \forall\ k$. Now,

$$\begin{aligned} R_j &= f_{j-1} R_0 + M^{-1} \dot{R}_{j-1} \\ \implies R_j^{(k)} &= (f_{j-1} R_0)^{(k)} + (M^{-1} \dot{R}_{j-1})^{(k)} \\ &= M^{-1} \dot{R}_{j-1}^{(k)} = M^{-1} R_{j-1}^{(k+1)}. \end{aligned}$$

  Using the the induction hypothesis it follows, $(R_0^\perp)^T R_j^{(k)} = 0 \forall\ k, j$.

Since $M^{(k)}(s_0) = 0; \quad s_0 \in \{0, 1\} \forall k$ on account of $\frac{d^k}{ds^k} \vec{B}(s_0) = 0; \quad s_0 \in \{0, 1\} \forall k$, the above result implies $R(1) || R_0(1)$ and $R(0) || R_0(0)$. Armed with this result, we use to Eq. A11 to arrive at a bound for $\mathcal{E}$ for two different cases, i.e, in absence and in presence of a thermal bath.

1. Absence of thermal bath

In absence of thermal bath M is anti-symmetric and consequently V is unitary. Thus, Eq. A11 reduces to

$$\left\| R^M(s) - R(s) \right\| \leq \epsilon^M \int_0^s ds' \left\| \dot{R}_M \right\|. \tag{A13}$$

Consider the expression $\|R(1) - R_0(1)\|$, using triangle inequality we can express,

$$\|R(1) - R_0(1)\| \leq \|R(1) - R^M(1)\| + \|R^M(1) - R_0(1)\|. \tag{A14}$$

Using $R^M(1) \| R_0(1)$ on account of all derivatives of $M(s)$ vanishing at $s = 1$,

$$\begin{aligned} \|R^M(1) - R_0(1)\| &= \|R_0 \| R^M(1)\| - R_0(1)\| \\ &= |\|R^M(1)\| - 1| \\ &\leq \|R^M(1) - R(1)\|, \end{aligned} \tag{A15}$$

where crucially, we have used $\|R(1)\| = 1$ as time-evolution is unitary for anti-symmetric M to go from the second to the last line on the LHS above.

Using Eq. A13 we get,

$$\|R(1) - R_0(1)\| \leq 2\epsilon^M \int_0^1 ds' \left\| \dot{R}_M \right\|. \tag{A16}$$

2. Presence of purely dephasing thermal bath

Again, using triangle inequality,

$$\|R(1) - R_0(1)\| \leq \|R(1) - R^N(1)\| + \|R^N(1) - R_0(1)\|. \tag{A17}$$

Using $R^N(1) \| R_0(1)$ on account of all derivatives of $M(s)$ vanishing at $s = 1$,

$$\begin{aligned} \|R^N(1) - R_0(1)\| &= \|R_0(1) \| R^N(1)\| - R_0(1)\| \\ &= |\|R^N(1)\| - 1| \\ &= |\epsilon f_0(1) + \epsilon^2 f_1(1) + \dots| \\ &\simeq \epsilon |f_0(1)| \\ \implies \|R(1) - R_0(1)\| &\simeq \epsilon |f_0(1)|. \end{aligned} \tag{A18}$$

Appendix B: Asymptotic behavior

We consider the error $\mathcal{E}$ in the presence of small but finite relaxation. To proceed it is useful to consider a matrix $V(s)$ with initial condition $V(0) = \mathbb{1}$, that satisfies

$$\dot{V} = \frac{1}{\epsilon} MV, \tag{B1}$$

where M is the matrix appearing in Bloch equation (Eq. 27). Using V we change to change to a new variable ξ,

$$\xi(s) = V^{-1}(s) R(s), \tag{B2}$$

that satisfies,

$$\epsilon \dot{\xi} = -4\beta \xi + 4\beta V^{-1} R_0. \tag{B3}$$

The solution to this equation is written as,

$$\begin{aligned} &\xi(s) = e^{-\frac{1}{\epsilon} \int_0^s 4\beta(s') ds'} \\ &\left(\int_0^s \frac{4\beta(s')}{\epsilon} e^{\frac{1}{\epsilon} \int_0^{s'} 4\beta(s'') ds''} V^{-1}(s') R_0(s') ds' + R(0) \right) \end{aligned} \tag{B4}$$

which in conjunction with Eq. B2, formally (i.e. contingent on having a solution for $V(s)$ in Eq. B1) solves the Bloch equation (Eq. 27). Note that Eq. B4 is completely consistent with our discussion in the $\beta = 0$ setting in Eq. B4 and using Eq. B2 leads to the solution $R(s) = V(s)R(0)$ where using Eq. B1 we find that R satisfies the same Bloch equation, Eq. 31 as used in previous section.

For finite relaxation, the first term in the parenthesis in Eq. B4 is non-zero and hence the matrix $V(s)$ (or equivalently $V^{-1}(s)$) must be known to calculate $R(1)$. However, $V(s)$ satisfying Eq. B1 with initial condition $V(0) = \mathbb{1}$

does not lend itself to a power series expansion in ϵ parallel to Eq. 32, invalidating the method used to obtain analytical solution for the Bloch vector in the previous section. Though there is no clear way to calculate the matrix $V(s)$ by solving Eq. B1, computing $\bar{R}$, the action of matrix $V(s)$ on the initial Bloch vector $R_0(0)$,

$$\bar{R} = V R_0(0) \tag{B5}$$

is analytically tractable. The solution for the vector $\bar{R}$ through Eq. 31 allows us to make an ansatz for $V(s)$ that leads to results consistent with numerics.

While a direct solution of V in Eq. B1 is difficult, we observe that the introduction of a finite relaxation does not change the solution for $\bar{R}$ in Eq. 31 except replacing $\alpha \to \alpha - \beta$. Therefore generalizing Eq. 40 we get, $\bar{R}(1) = f(s)R_0(1)$ where $f(s)$ is given by Eq. 36 but unlike previous section β is no longer assumed to be zero. Using Eq. B5, this relation can be used to constrain $V(s)$ according to the relation

$$V(1)R_0(0) = f(1)U_0(1)R_0(0) \tag{B6}$$

where we have used the relation $R_0(s) = U_0(s)R_0(0)$ where U_0 is defined in Eq. 44.This motivates our anstaz

$$V(s) \approx f(s)U_0(s) \tag{B7}$$

in Eq. B4 which interpolates correctly, satisfying the initial condition $V(0) = \mathbb{1}$ at $s = 0$ as well as Eq. B6 at $s = 1$. Note that, the above approximation satisfies $V(s) \to U_0(s)$ as $T \to \infty$.

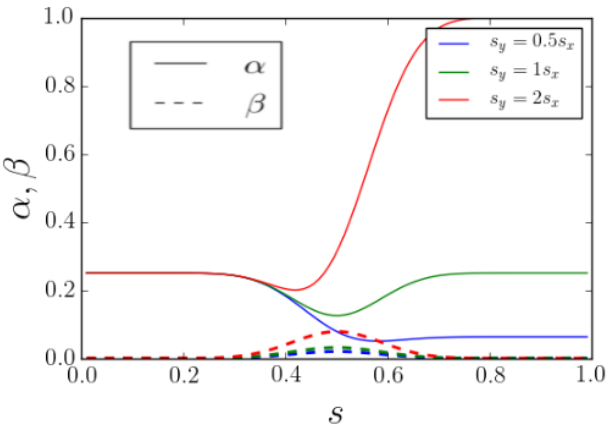

FIG. 6: Plot of effective dephasing (α) and relaxation (β) as a function of scaled time, s for system-bath coupling strength $s_x = 0.5$ and s_y given in the key. The dashed curve corresponds to effective relaxation, β and the solid curve corresponds to effective dephasing, α. The dephasing parameter, η_0 and the relaxation parameter η are chosen equal to each other and set to 1.

Substituting Eq. B7 in Eq. B4, we make the the following ansatz,

$$\begin{aligned} R(1) &= U_0 f(1) e^{-\frac{4}{\epsilon}\int_0^1 \beta} \left(\frac{4}{\epsilon} \int_0^1 \beta e^{\frac{4}{\epsilon}\int_0^s \beta} f^{-1}(s) + 1 \right) R(0) \\ &= \left(1 + f(1) \int_0^1 \left(\frac{d}{ds} f^{-1} \right) e^{-\frac{4}{\epsilon}\int_s^1 \beta} ds \right) R_0(1). \end{aligned} \tag{B8}$$

Restricting f and f^{-1} in the above formula to lowest order in ϵ , we get $\|R(1)\| = 1 + \int_0^1 \left(\frac{d}{ds} f_0^{-1}\right) e^{-\frac{4}{\epsilon}\int_s^1 \beta} ds$ where

$$f_0(s) = -\int_0^s \frac{(\alpha-\beta)\omega^2}{2(1+(\alpha-\beta)^2)}. \tag{B9}$$

As a consistency check note that Eq.B8 reduces to Eq, 40 in the limit $\beta \to 0$. Moreover, since R must be bounded in norm $\|R(1)\| \leq 1$, $\frac{(\alpha-\beta)\omega^2}{2(1+(\alpha-\beta)^2)} > 0$ must hold. This condition suggests the requirement $\alpha > \beta$ for the ansatz offered in Eq. B8 to hold. We point out that $\alpha > \beta$ condition can be satisfied provided the two system-bath coupling parameters have same order of magnitude, $s_x \sim s_y$ and dephasing strength is stronger than relaxation, $\eta_0 \geq \eta$. This is clear from the Fig. 6, where we plot effective relaxation and effective dephasing as defined in Eq. 25. The dephasing parameter, η_0 and the relaxation parameter, η are chosen as, $\eta_0 = \eta = 1$. For all the curves, $s_x = 0.5$. We have chosen to vary just s_y because both α and β are invariant under combined effect of reflection about $s = 0.5$ and $s_x \rightleftarrows s_y$ exchange. We see that for wide-ranging values of s_y, $\alpha(s) > \beta(s) \forall s \in [0, 1]$. Thus we conclude, for comparable values of system-bath coupling strengths, $s_x \sim s_y$, $\eta_0 > \eta$ is a good criterion to ensure $\alpha(s) > \beta(s) \forall s \in [0, 1]$.

Using Eq. B8, the error may be computed as

$$\begin{aligned} \mathcal{E}(T) = \|R(1) - R_0(1)\| &= f(1) \int_0^1 (\frac{d}{ds} f^{-1}) e^{-4T\int_s^1 \beta} ds \\ &\approx -\frac{1}{T} \int_0^1 \dot{f}_0 e^{-4T\int_s^1 \beta} ds, \end{aligned} \tag{B10}$$

with $\dot{f}_0 = \frac{(\alpha-\beta)\omega^2}{2(1+(\alpha-\beta)^2)}$ and α,β being defined according to Eq. 25.

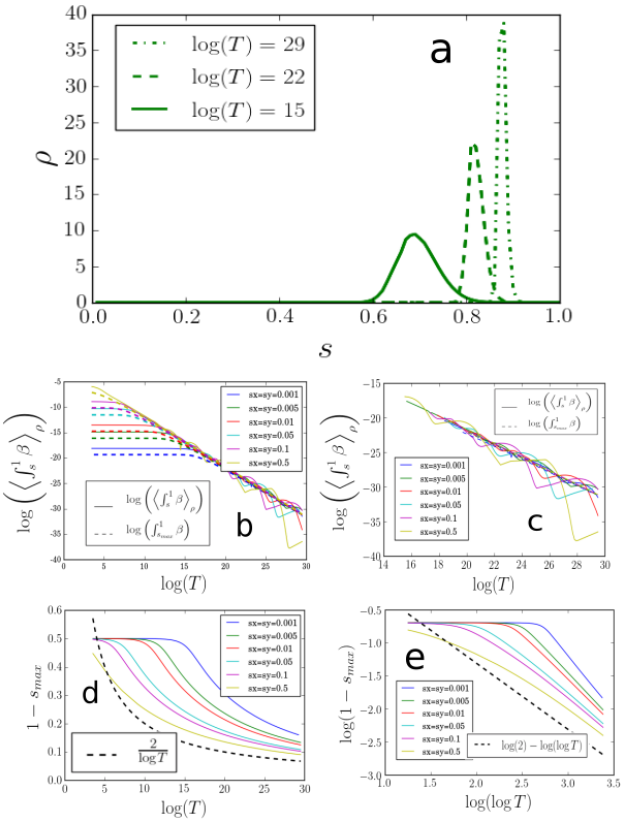

FIG. 7: (Panel a) Plot of ρ (Eq.B12) for different values of time T. The peak-height and the width of the probability density ρ is an increasing and a decreases function of T, respectively. The probability densities look identical at this scale for values of $s_x = s_y$ varied from 0.005 to 0.5 (i.e. over two orders of magnitude). (Panels b and c) Comparison of $\left\langle \int_s^1 \beta \right\rangle_\rho$ (defined by Eq. B13) , plotted in solid curves, versus its approximate estimate given by values of $\int_{s_{max}}^1 \beta$ as a function of total time T (in the units of $1/\Delta$), plotted in dashed curves, for different values of dephasing, α and relaxation strength, β characterized by the shown values of $s_x = s_y$ (see Eq. 27-26). Relaxation and dephasing parameters, η and η_0, that solely depend on bath Hamiltonian are both set to $\eta = \eta_0 = 1$. Both sets of curves, solid and dashed, are computed numerically. There exists a region, for small values of T, over which T dependence of $\left\langle \int_s^1 \beta \right\rangle_\rho$ vanishes (panel c). This region is well captured by the approximate formula $\int_{s_{max}}^1 \beta$, however the value of $\left\langle \int_s^1 \beta \right\rangle_\rho$ itself is underestimated by the formula. For large values of T, $\left\langle \int_s^1 \beta \right\rangle_\rho$ values tend to oscillate, however, the average slope is again well captured by the approximate formula $\int_{s_{max}}^1 \beta$ (top left panel).
(Panels d and e) Plot of $1 - s_{max}$ as a function of $\log T$ (bottom right panel) and the same plot in log-log scale is shown in bottom left panel. Notice that T independent region of $\left\langle \int_s^1 \beta \right\rangle_\rho$ corresponds to $s_{max} \approx 0.5$. $s_{max} \approx 0.5$ region ends in a kink beyond which $1 - s_{max}$ decreases zero, asymptotically approaching $\frac{1}{\log T}$. This asymptotic dependence is shown in the log-log plot in the bottom right panel.

Now, we estimate the exponent of T which governs the power-law dependence of $\|R(1) - R_0(1)\| = \mathcal{E}$ for large T. For our convenience we will restrict ourselves to the special case $s_x = s_y$, (see Eq. 27-26) essentially allowing the system bath coupling to be governed by a single parameter. Taking the derivative of $\log(\mathcal{E})$with respect to T,

$$\frac{d}{dT}\log(\mathcal{E}) \approx -\frac{1}{T} - \frac{4\int_0^1 ds \dot{f}_0 e^{-4T\int_s^1 \beta}\int_s^1 \beta}{\int_0^1 ds \dot{f}_0 e^{-4T\int_s^1 \beta}}. \quad \text{(B11)}$$

Defining,

$$\rho \equiv \frac{\dot{f}_0 e^{-4T\int_s^1 \beta}}{\int_0^1 \dot{f}_0 e^{-4T\int_s^1 \beta}} \quad \text{(B12)}$$

as a probability density defined over $[0, 1]$, the second term in the equation above is interpreted as

$$\left\langle 4\int_s^1 \beta \right\rangle_\rho \equiv \frac{4\int_0^1 ds \dot{f}_0 e^{-4T\int_s^1 \beta}\int_s^1 \beta}{\int_0^1 ds \dot{f}_0 e^{-4T\int_s^1 \beta}}. \quad \text{(B13)}$$

The function $\dot{f}_0(s) = -\frac{(\alpha-\beta)\dot{\theta}^2}{2(1+(\alpha-\beta)^2)}$ (Eq. B9), is symmetric about $s = 0.5$ (when $s_x = s_y$) and exponentially goes to zero at $s = 1$, while, the function $e^{-4T\int_s^1 \beta}$ is an increasing function over $[0, 1]$ where, it decreases exponentially from the value 1 at $s = 1$ to the value $e^{-4T\int_0^1 \beta}$ at $s = 0$ with exponent being proportional to T. These properties imply that ρ is a sharply peaked (see Fig. 7a) distribution for large T (defining large T when $1/T \ll \int_0^1 \beta$ holds) with the maximum value $\rho_{max} = \rho(s_{max})$ for $s_{max} \in (0.5, 1)$. Moreover, $s_{max} \to 1$ as $T \to \infty$. Hence for large value of T, we approximate (see Fig. 7),

$$\left\langle \int_s^1 \beta \right\rangle_\rho \simeq \int_{s_{max}}^1 \beta. \quad \text{(B14)}$$

s_{max} is the solution to the equation $\rho'(s)|_{s_{max}} = 0$,

$$0 = \frac{\dot{\Omega}}{\Omega} + 2\frac{\dot{\omega}}{\omega} + 4T\beta\Big|_{s_{max}} \quad \text{(B15)}$$

where, we defined $\Omega \equiv \frac{(\alpha-\beta)}{2(1+(\alpha-\beta)^2)}$ and $\omega = \dot{\theta}$ (see Eq. 11) for brevity. Since $\Omega(s \to 1) \neq 0$ and $\Omega'(s \to 1) = 0$, we conclude $\left|\frac{\dot{\Omega}}{\Omega}\right| \ll \left|\frac{\dot{\omega}}{\omega} = -\frac{2s-1}{s^2(1-s)^2}\right|$ for $s \to 1$. Thus, neglecting $\frac{\Omega'}{\Omega}$ term in the Eq. B15, the equation for s_{max} in the $T \to \infty$ limit is given by

$$\frac{2s_{max} - 1}{4T} \simeq \frac{1}{2}s_{max}^2(1 - s_{max})^2\beta(s_{max}). \quad \text{(B16)}$$

This result immediately leads to two conclusions. First, using the asymptotic form of β,

$$\beta \overset{s\to 1}{\simeq} \eta\left(\frac{\pi}{4C}\right)^2 (s_x^2 + s_y^2)s^4(1 - s)^4 e^{-\frac{2}{1-s}}, \quad \text{(B17)}$$

where $C \equiv \int_0^1 ds' e^{-1/s'(1-s')}$, one finds $\log(T) \sim \frac{2}{1-s_{max}} + O(\log(1 - s_{max}))$, and thus,

$$s_{max} \sim 1 - \frac{2}{\log(T)}. \quad \text{(B18)}$$

Second, using asymptotic dependence of $\int_s^1 \beta$ on s given by,

$$\int_s^1 \beta ds \overset{s\to 1}{\simeq} \frac{1}{2}s^2(1 - s)^2\beta(s). \quad \text{(B19)}$$

Taken together with Eq. B16, we get

$$\frac{2s_{max}-1}{4T} \simeq \int_{s_{max}}^{1} \beta ds. \tag{B20}$$

Thus,

$$\begin{aligned}\frac{1}{\mathcal{E}}\frac{d\mathcal{E}}{dT} &\approx -\frac{1}{T} - \left\langle 4\int_{s}^{1} \beta ds \right\rangle \\ &\simeq -\frac{1}{T} - 4\int_{s_{max}}^{1} \beta ds \\ &\simeq -\frac{2s_{max}}{T}. \end{aligned} \tag{B21}$$

In conclusion, $\|R(1) - R_0(1)\|$ is given by

$$\|R(1) - R_0(1)\| \sim T^{-2s_{max}}. \tag{B22}$$

Defining the exponent at time T as

$$m(T) \equiv -2s_{max} \sim -2 + \frac{4}{\log T}, \tag{B23}$$

where we have used the asymptotic dependence of s_{max} on T (see Eq. B18). Since $s_{max}(T) \in (0.5, 1)$, the exponent $m(T) \in (1, 2)$ with $m(T \to \infty) = 2$. All assumptions leading upto this result are verified against exact numerical results in Fig. 7.

[1] T. Karzig, Y. Oreg, G. Refael, and M. H. Freedman, Physical Review X **6**, 031019 (2016).
[2] B. Van Heck, A. Akhmerov, F. Hassler, M. Burrello, and C. Beenakker, New Journal of Physics **14**, 035019 (2012).
[3] T. Hyart, B. Van Heck, I. Fulga, M. Burrello, A. Akhmerov, and C. Beenakker, Physical Review B **88**, 035121 (2013).
[4] Chetan Nayak, Steven H. Simon, Ady Stern, Michael Freedman, and S. Das Sarma., Rev. Mod. Phys. **80**, 1083 (2008).
[5] Alexei Kitaev, arXiv:cond-mat/0010440 (2000).
[6] C. W. J. Beenakker, Annu. Rev. Con. Mat. Phys. **4**, 113 (2013).
[7] Roman M. Lutchyn, Jay D. Sau, and S. Das Sarma., Phys. Rev. Lett. **105**, 077001 (2010).
[8] Yuval Oreg, Gil Refael and Felix von Oppen., Phys. Rev. Lett. **105**, 177002 (2010).
[9] M. Cheng, R. M. Lutchyn, and S. D. Sarma, Physical Review B **85**, 165124 (2012).
[10] V. Mourik, K. Zuo, S. M. Frolov, S. R. Plissard, E. P. A. M. Bakkers and L. P. Kouwenhoven., Science **336**, 1003 (2012).
[11] Leonid P Rokhinson, Xinyu Liu, and Jacek K Furdyna., Nat. Phys. **8**, 795 (2012).
[12] A. D. K. Finck, D. J. Van Harlingen, P. K. Mohseni, K. Jung, and X. Li, Phys. Rev. Lett **110**, 126406 (2013).
[13] Anindya Das, Yuval Ronen, Yonatan Most, Yuval Oreg, Moty Heiblum and Hadas Shtrikman., Nat. Phys. **8**, 887 (2012).
[14] H. O. H. Churchill, V. Fatemi, K. Grove-Rasmussen, M. T. Deng, P. Caroff, H. Q. Xu, and C. M. Marcus., Phys. Rev. B **87**, 241401 (2013).
[15] S. M. Albrecht, A. Higginbotham, M. Madsen, F. Kuemmeth, T. S. Jespersen, J. Nygård, P. Krogstrup, and C. Marcus, Nature **531**, 206 (2016).
[16] M. Deng, S. Vaitiekėnas, E. B. Hansen, J. Danon, M. Leijnse, K. Flensberg, J. Nygård, P. Krogstrup, and C. M. Marcus, Science **354**, 1557 (2016).
[17] H. Zhang, Ö. Gül, S. Conesa-Boj, K. Zuo, V. Mourik, F. K. de Vries, J. van Veen, D. J. van Woerkom, M. P. Nowak, M. Wimmer, et al., Nature Nanotechnology (2018).
[18] J. Alicea, Y. Oreg, G. Refael, F. Von Oppen, and M. P. Fisher, Nature Physics **7**, 412 (2011).
[19] J. D. Sau, D. J. Clarke, and S. Tewari, Physical Review B **84**, 094505 (2011).
[20] M. Cheng, V. Galitski, and S. D. Sarma, Physical Review B **84**, 104529 (2011).
[21] T. Karzig, G. Refael, and F. von Oppen, Physical Review X **3**, 041017 (2013).
[22] M. S. Scheurer and A. Shnirman, Physical Review B **88**, 064515 (2013).
[23] C. Knapp, M. Zaletel, D. E Liu, M. Cheng, P. Bonderson, and C. Nayak, Physical Review X **6**, 041003 (2016).
[24] Bauer, Bela and Karzig, Torsten and Mishmash, Ryan V. and Antipov, Andrey E. and Alicea, Jason, arXiv:1803.05451 (2018).
[25] F. L. Pedrocchi and D. P. DiVincenzo, Physical review letters **115**, 120402 (2015).
[26] G. Goldstein and C. Chamon, Physical Review B **84**, 205109 (2011).
[27] D. Rainis and D. Loss, Physical Review B **85**, 174533 (2012).
[28] F. Konschelle and F. Hassler, Physical Review B **88**, 075431 (2013).
[29] F. L. Pedrocchi, N. Bonesteel, and D. P. DiVincenzo, Physical Review B **92**, 120402 (2015).
[30] A. M. Childs, E. Farhi, and J. Preskill, Physical Review A **65**, 012322 (2001).
[31] W. Yao, R.-B. Liu, and L. Sham, Physical review letters **98**, 077602 (2007).
[32] A. J. Leggett, S. Chakravarty, A. Dorsey, M. P. Fisher, A. Garg, and W. Zwerger, Reviews of Modern Physics **59**, 1 (1987).
[33] U. Weiss, *Quantum dissipative systems*, vol. 13 (World scientific, 2012).
[34] E. Brian Davies, Math. Phys **39**, 91 (1974).
[35] H.-P. Breuer and F. Petruccione, *The theory of open quantum systems* (Oxford University Press on Demand, 2002).
[36] J. Preskill, Lecture notes for Physics 219: Quantum computation (1999).
[37] T. Albash and D. A. Lidar, Physical Review A **91**, 062320 (2015).
[38] N. Wiebe and N. S. Babcock, New Journal of Physics **14**, 013024 (2012).
[39] D. A. Lidar, A. T. Rezakhani, and A. Hamma, Journal of Mathematical Physics **50**, 102106 (2009).
[40] A. Joye and C.-E. Pfister, Journal of Physics A: Mathematical and General **24**, 753 (1991).
[41] G. Nenciu, Communications in mathematical physics **152**, 479 (1993).
[42] G. A. Hagedorn and A. Joye, Journal of mathematical analysis and applications **267**, 235 (2002).
[43] T. Karzig, F. Pientka, G. Refael, and F. von Oppen, Physical Review B **91**, 201102 (2015).
[44] J. D. Sau, S. Tewari, and S. D. Sarma, Physical Review A **82**, 052322 (2010).
[45] D. J. Clarke, J. D. Sau, and S. D. Sarma, Physical Review X **6**, 021005 (2016).
[46] D. Aasen, M. Hell, R. V. Mishmash, A. Higginbotham, J. Danon, M. Leijnse, T. S. Jespersen, J. A. Folk, C. M. Marcus, K. Flensberg, et al., Physical Review X **6**, 031016 (2016).